Impedance Measurements of Motor Drives and Supplies in NASA NEAT Facility

Timothy P. Dever[†], David J. Sadey[*], Keith Hunker[†], Xavier Collazo[*], Patrick Hanlon[*], Peter E. Kascak[†], Casey Theman[‡], Brian P. Malone[*]
NASA Glenn Research Center, Cleveland, OH, 44135

Many electrified aircraft configurations consist of a number of power components operating on the same shared electrical bus. Understanding the impedance performance of electrical loads and sources is key to understanding, and designing for, acceptable overall vehicle power quality and power system stability. This paper discusses impedance measurements made on the NASA Electric Aircraft Testbed (NEAT) Electrical Power System (EPS) at NASA Glenn Research Center. First, an overall discussion of the NEAT facility configuration during testing is presented. Then, details of the impedance measurement approach and the various testing configurations are discussed. Next, input impedance measurements at NEAT, including sources (DC supplies) and loads (multiple motor drives, electric machines, and resistive load banks, with long interconnecting cable leads), are performed under a number of conditions, and results, including load model comparisons and stability analysis, are presented and discussed.

I. Nomenclature

EPS	=	Electrical Power System
EAP	=	Electrified Aircraft Propulsion
HIL	=	Hardware in the loop
IMS	=	Impedance Measurement System
NASA	=	National Aeronautics and Space Administration
NEAT	=	NASA Electric Aircraft Testbed
TEEM	=	Turbine Electrified Energy Management
Z	=	Impedance

II. Introduction

The NASA Electric Aircraft Testbed (NEAT) is located at NASA Glenn Research Center (GRC), specifically at the Neil A. Armstrong Test Facility (ATF) in Sandusky, Ohio. NEAT has been developed with the goal of providing a testbed to enable end-to-end testing of technologies required in the development of megawatt (MW) Electrical Aircraft Propulsion (EAP) systems at power and altitude [1]. The NEAT facility consists of numerous electric machines (permanent magnet synchronous motors), machine drives, DC supplies, and resistive load banks, connected over long leads in an attempt to mimic megawatt EAP aircraft electrical power systems (EPS). The purpose of these measurements is to understand the impedance performance of electrical loads and sources, in order to understand, and design for, acceptable overall vehicle power quality and power system stability. This paper will describe the test setup of, and present results from, impedance measurements of supplies and loads (drives and electric machines, in motor and generator mode, and resistive load banks) under a number of conditions.

NEAT was designed to be a reconfigurable facility. In Section III, an overview of the NEAT facility configuration at the time of testing is presented. In Section IV, specifics of the impedance measurement process, including the

[*] Electrical Engineer, Power Management and Distribution Branch, 21000 Brookpark Rd MS 301-5.
[†] Electrical Engineer, Diagnostics and Electromagnetics Branch, 21000 Brookpark Rd MS 309-2.
[‡] Electrical Engineer, Space Power and Propulsion Test Engineering Branch, 21000 Brookpark Rd MS 333-1.

hardware, measurement approach, and limitations are discussed. Section V covers the detailed testing (source and load) configurations. In Section VI, the measured impedance data for the loads and sources is presented. In Section VII, a load impedance model of the NEAT power system is developed and compared to the measured impedance data. In Section VIII, a stability analysis of the NEAT EPS is performed and discussed. This paper is a companion to [2], which discusses low power testing in NASA's SPEED Testbed.

III. NEAT Test Facility

The NEAT facility is, by design, a reconfigurable facility. For the measurements reported in this paper, the NEAT EPS was configured for hardware in the loop (HIL) testing of an advanced turbine control strategy called Turbine Electrified Energy Management (TEEM), as described in [3]. A schematic of the EPS configuration during these tests is shown in Fig. 1.

The NEAT EPS includes eight 250 kW permanent magnet synchronous machines (PMSM), four each on two common shafts. Each PMSM is driven and controlled by a motor drive with a built-in controller; thus each circle designated M1-M8 in the figure depicts a combined machine and drive. The DC side of the drives for a pair of machines on each shaft is connected to a DC bus common to a second pair of drives, operating machines on the other shaft. Under standard operation, each DC bus is operated at 700 V and is supplied by three-250 kW unidirectional power supplies, which regulate the busses. Also included on each bus is a reconfigurable load bank (1 MW capability), and a safety brake module, which is disengaged under nominal operation. Test Points labelled '1' and '2' in the figure are the measurement points, and are discussed in the Measurement Configurations section.

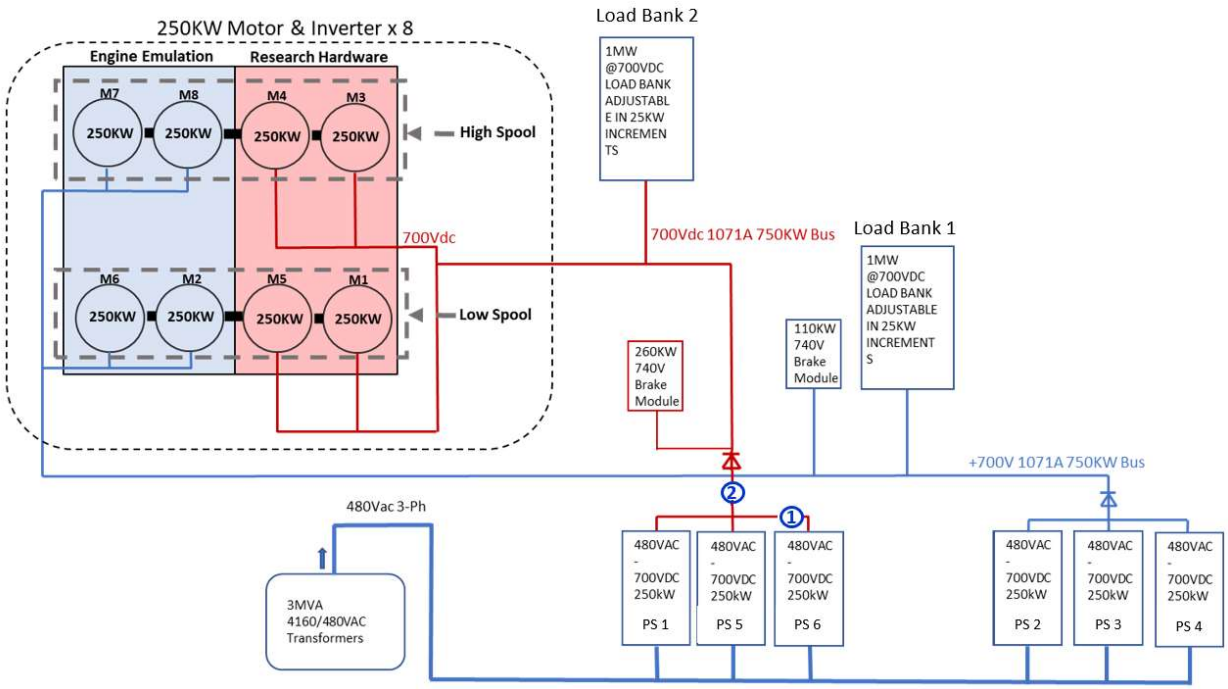

Fig. 1. Schematic of the NEAT facility EPS configuration during TEEM testing

IV. Impedance Measurement Details

This section covers the specifics of the impedance measurements performed. A simplified schematic describing the measurement configuration is detailed in Fig. 2. Relevant components are the source (V_{supply}), the impedance measurement equipment (IMS; transformer; and voltage and current measurements, labelled in blue), and the load (drive and PMSM). The IMS consists of a control computer and a Frequency Response Analyzer (FRA). The IMS generates low level sinusoidal test signals swept over the desired frequency range, and includes a power amplifier to amplify these signals, as well as analog inputs, and software which performs the impedance calculations. The transformer is used to inject the signals from the power amplifier. Voltage and current measurements are fed into the IMS for impedance calculations. During testing, both load and source impedances were measured. Current measurements (I_{IMS}) are common to both impedance load and source measurements; source voltage (V_{IMS} source) is measured on the source side of the transformer, and load voltage (V_{IMS} load) is measured on the load side of the transformer.

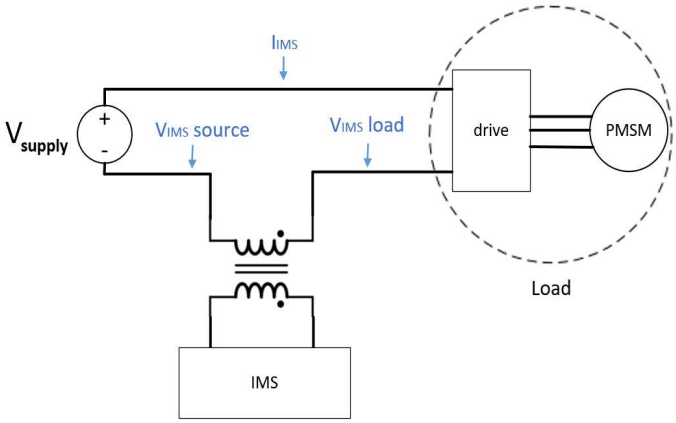

Fig. 2 Schematic of IMS implementation

The IMS posed several operational limitations. Firstly, although NEAT is a high power facility, the IMS is a lower power unit. Because voltage and current levels during nominal NEAT operation would exceed the safe transformer operational limits, care was taken to avoid exceeding these limits during the impedance measurements. These constraints were built into the test plan, and the DC bus was limited to 300 volts during measurements. Secondly, the transformer bandwidth was limited, which placed restrictions on the frequency range of the testing: test signal sweep frequency range (and therefore the resulting impedance data) was kept between 100 Hz and 50 kHz. However, this limitation did not appear to impact the goals of this effort, as system behavior of interest for the modeling and stability analyses appears to be limited to this range. In parallel to this measurement effort, development of impedance measurement capability at higher power and over wider frequency ranges is also being performed at NASA GRC, as discussed in [4].

An additional operational restriction was imposed due to the wide variation in the impedances of the systems under test. Due to very low load impedances at certain frequencies, signal injection voltage was limited to a desired range: a swept voltage signal high enough to develop sufficient current for a quality impedance measurement, but not so high that resulting currents were too large. Large currents might result in poor quality measurements, or worse, damage the measurement equipment. Accordingly, care was taken to limit test current, using an experimental approach: starting with a very low signal level injection, the test signal was swept over the desired frequency range; currents were monitored during the entire sweep to ensure that they were kept under desired limits; and calculated impedance results were checked to ensure that sufficient signal was captured to allow for quality data. Using this iterative approach, a single input signal size was found to be sufficient for the entire frequency range – meaning dual frequency range testing, which was implemented in [2], was not required.

V. Measurement Configurations

Measurements were made on a subset of the NEAT facility hardware; specifically, on the loads and sources in the "Research Hardware" portion of the facility (Fig. 1). Sources under test were DC supplies PS 1, PS 5, and PS 6. Loads tested included motor/drive systems M1 and M3, and Load Bank 2. Sources and loads from the "Engine Emulation" section were used to exercise the equipment under test, and included PS 2, PS 3, and PS 4; and M2, M8, and Load Bank 1. The brake modules were out of the circuit during testing; and M4, M5, M6 an M7 were disabled throughout.

Impedance measurements were taken at two distinct points in the system, labelled '1' and '2' in Fig. 1. In order to perform the measurements, a break needed to be made in the power cable, to allow insertion of the transformer for signal injection.

In both measurement positions, source and load impedance measurements were made. A number of conditions were tested. At Test Point 1, a single power supply was measured (PS 6; the other two supplies, PS1 and PS5, were disconnected for the test); in Test Point 2 the three supplies were measured in parallel. In each of these locations, three different test configurations were measured: a resistive load only (using Load Bank 2, a reconfigurable load); a single PMSM in motor mode; and a single PMSM in generator mode, with appropriate resistive load added to the bus to absorb the generated power. Additionally, at Test Point 2, a measurement was made using two machines (M1 and M3, on the same bus but on different shafts); one in motor mode, and one in generator mode.

A complete list of the completed Test Configurations is included in Table 1. A list of the reconfigurable Load Bank Configurations is provided in Table 2.

Table 1 Test Configurations

Test Points	Test Case	Load Bank 1	Load Bank 2	M3	M8	M1	M2	condition	test description
1	1	Disabled	Step 1, 1+2. 1+2+3	Disabled	Disabled	Disabled	Disabled	1 = 20 ohms; 15 A	single Magna supply driving loadbank
	2							1+2+3 = 5 ohms, 60 A	
	3							1+2 = 10 ohms, 30 A	
	4	Step 4+1	Disabled	2500 RPM	Walk up torque to obtain 20, 40, and 60A.	Disabled	Disabled	M3 = 2500 rpm; M8 = 0 Nm; Idc = 23 A	single Magna supply driving single drive and motoring machine
	5							M3 = 2500 rpm; M8 = -15 Nm; Idc = ~40	
	6							M3 = 2500 rpm; M8 = -40 Nm; Idc = ~65 A	
	-	Disabled	Step 1+2+3	Walk up torque to obtain 20, 40, and 50A.	2500 RPM	Disabled	Disabled	M3 = 0 Nm; M8 = 2500 rpm; Idc = 60 A (not run; duplicate of Test 2	single Magna supply driving single drive and generating machine (+ load bank to keep current positive)
	7							M3 = -20 Nm; M8 = 2500 rpm; Idc = 40 A	
	8							M3 = -45 Nm; M8 = 2500 rpm; Idc = 22 A	
2	9	Disabled	Step 1, 1+2. 1+2+3	Disabled	Disabled	Disabled	Disabled	1 = 20 ohms; 15 A	Three Magna supplies driving loadbank
	10							1+2 = 10 ohms, 30 A	
	11							1+2+3 = 5 ohms, 60 A	
	12	Step 4+1	Disabled	2500 RPM	Walk up torque to obtain 20, 40, and 60A.	Disabled	Disabled	M3 = 2500 rpm; M8 = 0 Nm; Idc = 22 A	Three Magna supplies driving single drive and motoring machine
	13							M3 = 2500 rpm; M8 = -15 Nm; Idc = 40 A	
	14							M3 = 2500 rpm; M8 = -40 Nm; Idc = 65 A	
	-	Disabled	Step 1+2+3	Walk up torque to obtain 20, 40, and 50A.	2500 RPM	Disabled	Disabled	M3 = 0 Nm; M8 = 2500 rpm; Idc = 60 A (not run; duplicate of Test 2	Three Magna supplies driving single drive and generating machine (+ load bank to keep current positive)
	15							M3 = -20 Nm; M8 = 2500 rpm; Idc = 40 A	
	16							M3 = -45 Nm; M8 = 2500 rpm; Idc = 22 A	
	17	Step 1	Disabled	2500 RPM	-15 Nm (40 A)	step torque to 35 A generated	2500 RPM		

Table 2 Load Bank Configurations

Step	Power (kW)	Resistance (Ω)	Step	Power (kW)	Resistance (Ω)
1	25	19.6	7	100	4.9
2	25	19.6	8	100	4.9
3	50	9.8	9	100	4.9
4	100	4.9	10	100	4.9
5	100	4.9	11	100	4.9
6	100	4.9	12	100	4.9

VI. Measured Impedance Data

Source and load impedance measurements were taken under all of the configurations described in Table 1. Test cases were selected in an effort to test interesting conditions; single-supply (Test Point 1) and three-supply (Test Point 2) configurations driving resistive loads only; and machines in both motor, and generator modes. Additionally, in the final three-supply case (Test 17) machines in motor (M3) and generator (M1) modes were tested on the same bus. However, under the measurement conditions achievable given the limitations of the impedance measurement equipment (frequency range limited to 100-50 kHz; and the relatively low power levels: maximum of 20 kW on a 1 MW system), measured system behavior did not change within either Test Point. The only configuration change that impacted measured source and load impedance was the choice of Test Point; i.e. the single-source data is notably different than the three-source data.

Measured source and load impedance data for all of the single-supply tests (Test Point 1, Cases 1-8) is plotted in Fig. 3; and impedance data for all three-supply tests (Test Point 2, Cases 9-17) is plotted in Fig. 4.

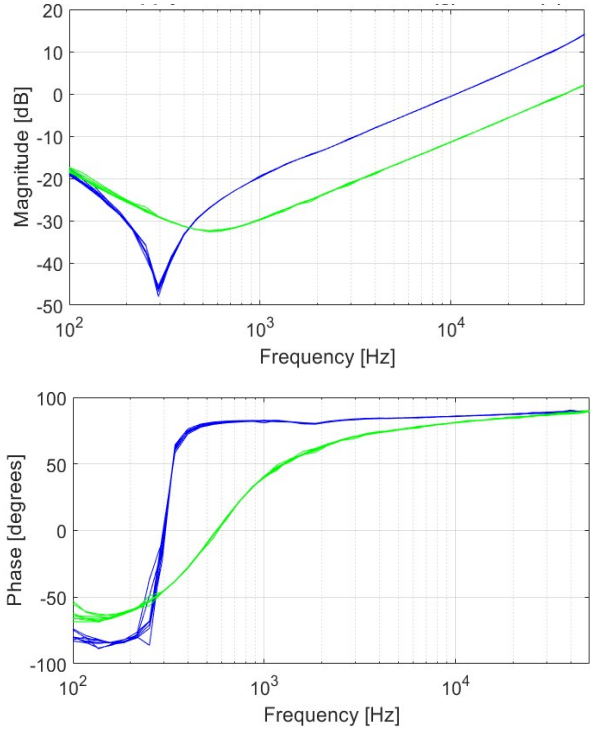

Fig. 3 Measured source Z (green) and load Z (blue), one-supply configuration

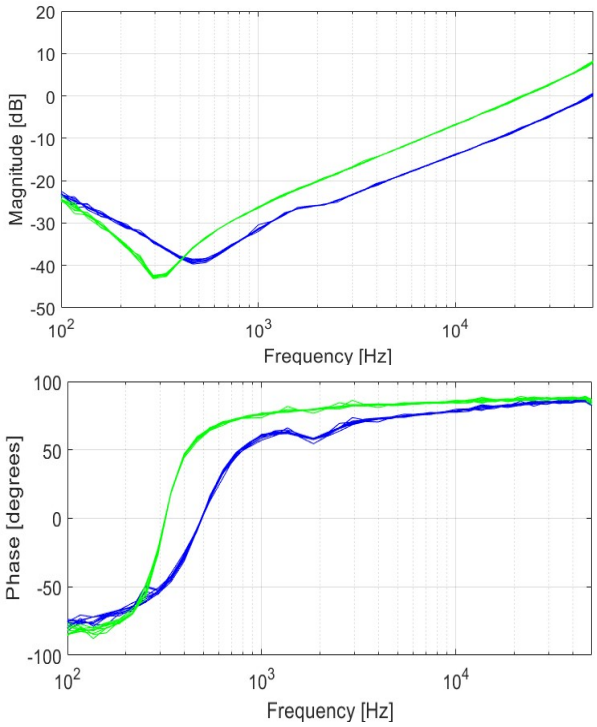

Fig. 4 Measured source Z (green) and load Z (blue), three-supply configuration

Note the similarity in the source and load impedances measured within Fig. 3 and Fig. 4; the measured data for each Test Case (i.e. single-supply or three-supply) overlap very closely. This similarity demonstrates that, at least under the measurement conditions achievable given the limitations of the impedance measurement equipment (frequency range limited to 100-50 kHz; and the relatively low power levels: maximum of 20 kW on a 1 MW system), system behavior did not change within a given Test Point.

Note that both sets of plots appear similar in structure. At lower frequencies, the source and load plots look capacitive (magnitude decreasing at 20 dB per decade, and phase approaching -90°); and at higher frequencies, the plots look inductive (magnitude increasing at 20 dB per decade, and phase approaching +90°).

However, the single-source data is notably different than the three-source data; e.g., note the variations in resonance point locations. This variation is expected because the sources and loads vary between the two configurations. As is discussed in the next section, due to limitations in the facility, the test point locations vary greatly: a long set of cables is included with the load in the one-supply configuration, and is included with the source in the three-supply configuration. When comparing Fig 4 versus Fig 3, we do expect a larger capacitance in the three-source case, given the combined output capacitance of three supplies, and the measurement does reflect this.

Additionally, the expected source inductance increase and load inductance decrease in the three-supply sources (due to relocation of the long leads in this configuration) are also present in the measured data.

It is worth noting that at lower frequencies, the magnitude of the impedance of the drive/motor combination (which acts as a constant power load) is expected to decrease with increased delivered power; and the phase angle is predicted to move from -90° to -180° [5]. Also note that the structure of the drive/machine impedance is consistent with that predicted [6].

VII. Model Development and Comparison

In this section, a load impedance model of the NEAT power system is first developed. This impedance model is then compared to the measured impedance data.

The supplies, drives, and load in the NEAT facility are connected via long lengths of cable. The model developed here follows the basic approach described in [6], with some modifications. Firstly, the facility schematic used was updated to reflect the changes made for the NEAT TEEM testing; and secondly, the model implementation was modified to enable comparison between simulated and measured data.

The first step in developing the load model was to develop representative schematics of the relevant components under test conditions. These schematics for the single-supply and the three-supply cases are presented in Fig. 5.

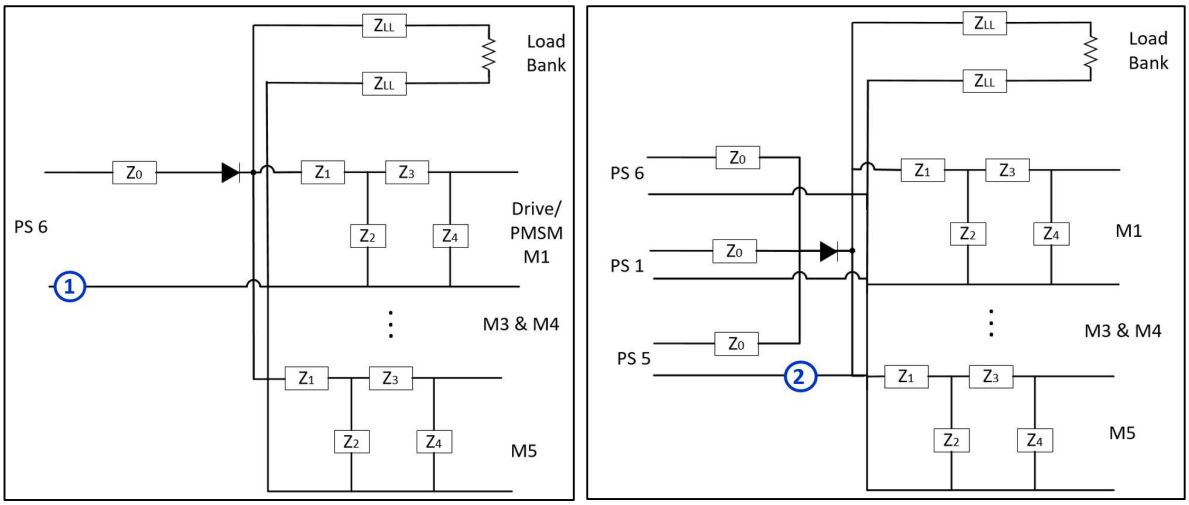

Fig. 5 NEAT schematic: single-supply (left) and three-supply configurations

Referring to Fig. 5, model impedances Z_0, Z_1, Z_3, and Z_{LL} describe the long cable runs in the system; during the NEAT TEEM testing, these cable lengths were 72, 54, 40, and 70 feet long, respectively. Impedances Z_2 and Z_4 describe capacitances along the line and at the motor drive DC inputs, respectively. Load bank resistances were selectable as defined in Table 2. Per Table 1, only a subset of the four drives and electric machines in the Research Hardware section were ever operated during testing; however, since the capacitors at the DC input to the drives were always in the circuit, all lines to the drives needed to be included in the model. Note that Test Point 1, the single-supply measurement, was located very close to the output terminals of the supply. Unfortunately, this was not possible for the three-supply configuration, because the supplies are interconnected at the end of a long (72') cable length, at the diode (see Test Point 2 in Fig 5), which results in this long cable length being included with the load in the single-supply measurements, and with the source in the three-supply measurements. Note that, in both Test Points, the transformer was inserted into the facility circuit on the low voltage side.

Cabling impedance estimates were calculated using known line lengths, along with estimates of per-foot estimates of cable resistance (manufacturer specified) and cable inductance (estimated parameter). These impedance estimates were combined with rated capacitance values, and built into a facility load impedance model. The model was then implemented in a Matlab script, which was run at a number of frequencies in the range of interest; results were then used to generate a Bode plot of the estimated load impedance. Using this approach, the model prediction could be directly compared to measured data.

The simulation was run in all of the test cases presented in Table 1. Example impedance model plots simulating Test Cases 2 (single-supply) and 11 (three-supply), along with the load impedances measured under those configurations, are plotted in Fig. 6 and Fig. 7.

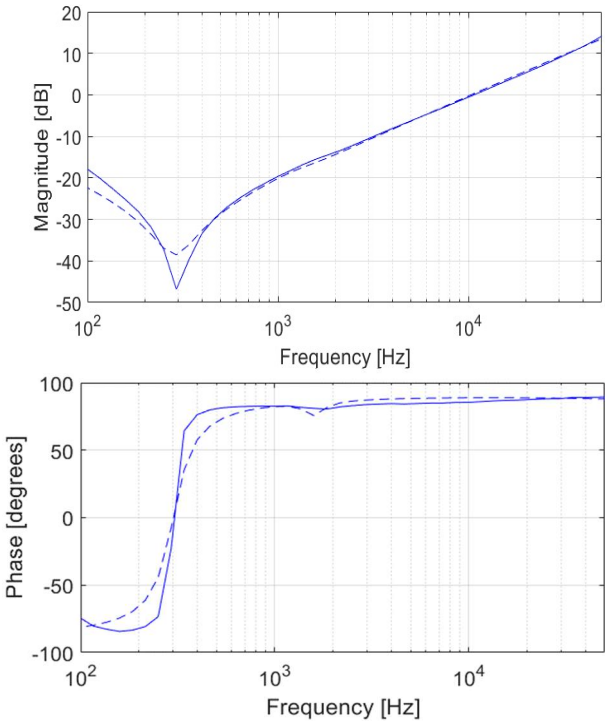

Fig. 6 Load Z measured (solid) and model (dashed), one-supply configuration

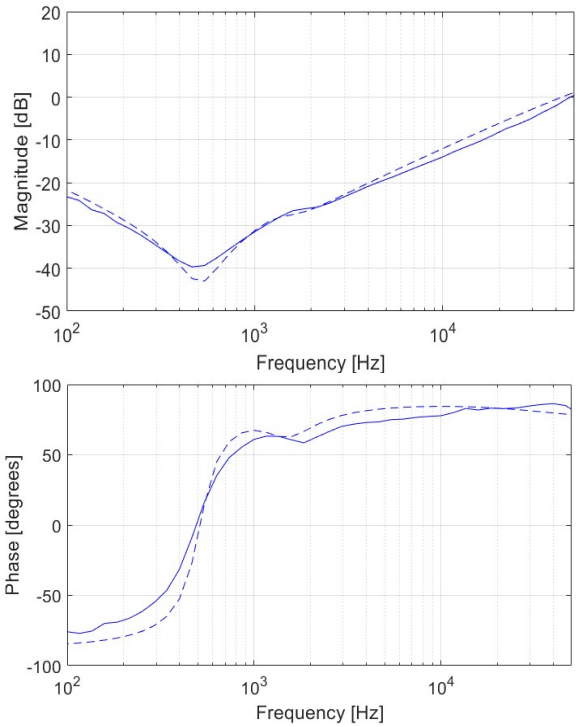

Fig. 7 Load Z measured (solid) and model (dashed), 3-supply configuration

Note that the models in Fig. 6 and Fig. 7 match the measured load impedance data fairly closely; appearing capacitive at low frequencies and inductive at high frequencies, with resonant points at the frequency locations consistent with the measurements. This provides some confidence that the relevant behavior of the NEAT loads has been captured within the frequency band measured. In future work, these models could be used in stability studies for new NEAT EPS configurations.

VIII. Stability Analysis

In this section, measured NEAT load and source impedances are used to perform a stability analysis on the system. This analysis was done on data for both the single-supply and three-supply configurations. Representative data (from Test Cases 1 and 9) are plotted in Figs 8 and 9. Stability assessments were not part of the original design effort for the NEAT lab; however, to assist in analysis, arbitrary stability margins (6 dB and 45°) were selected, and Nyquist plots of Z_S/Z_L were done, shown in Figs 10 and 11.

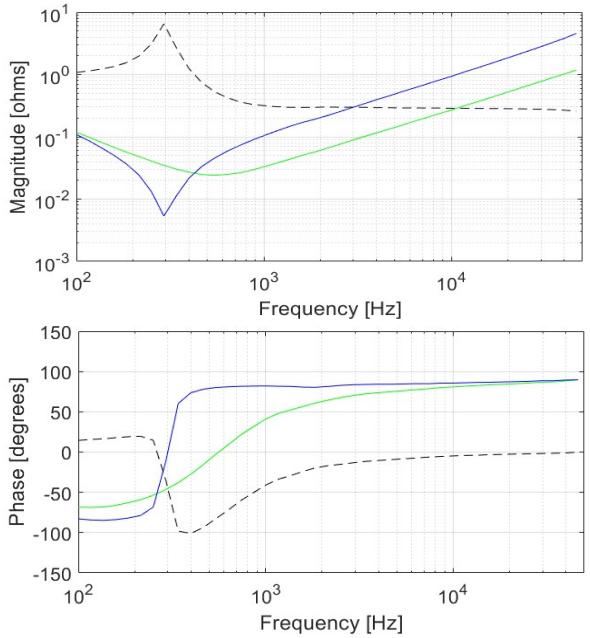

Fig. 8 1-supply case: measured source Z (green), load Z (blue); $|Z_S/Z_L|$ (top dashed), phase angle difference (bottom dashed)

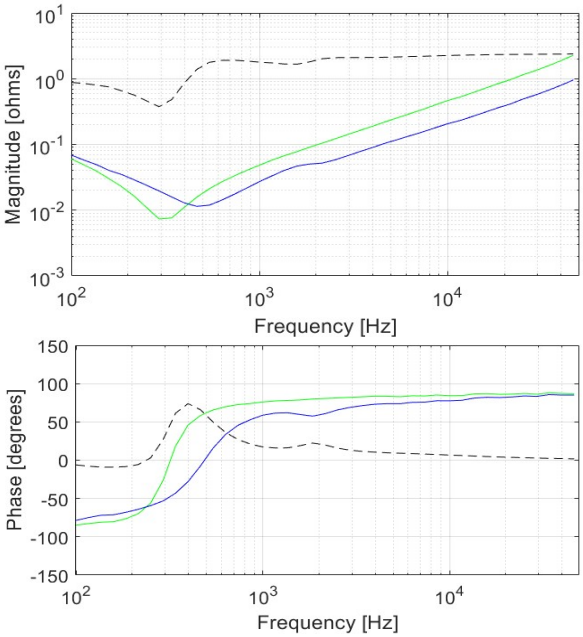

Fig. 9 3-supply case: measured source Z (green), load Z (blue); $|Z_S/Z_L|$ (top dashed), phase angle difference (bottom dashed)

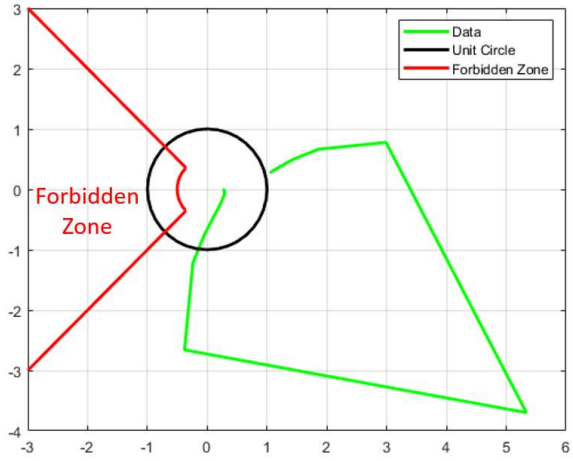

Fig. 10 Z_S/Z_L Nyquist plot, 1-supply case

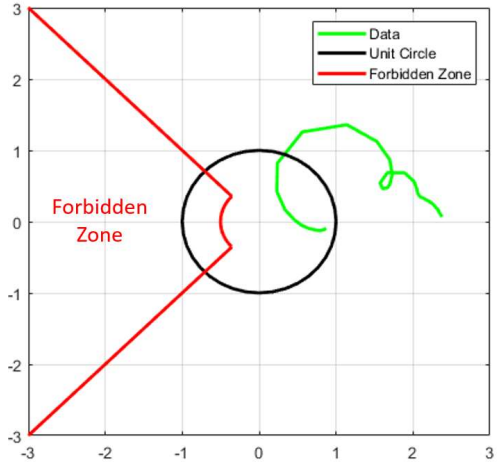

Fig. 11 Z_S/Z_L Nyquist plot, 3-supply case

In Fig. 8 and Fig. 9, source impedances (Z_S) and load impedances (Z_L) are plotted together. Additionally, in the top plots $|Z_S/Z_L|$ is plotted (dashed line), and in the bottom plots, the difference between the source and load impedance phase angles is plotted (dashed line). Inspecting these plots, no stability issues are anticipated based on the measured data: angle differences would need to exceed 135° (given a 45° margin) to ever fail the stability criteria, and the largest difference measured is only 100° (in Fig. 8). The Nyquist plots bear this out; in both Fig. 10 and Fig. 11, the plotted data remains out of the Forbidden Zone imposed by the stability criteria. These results are consistent with the observations; no marginal stability or instability issues were observed on the DC bus while the test measurements were taken. Of course, these results are limited by the available measured data. As was mentioned previously, the magnitude and phase of the drive/motor impedance is expected to change at lower frequencies; the magnitude decreasing from purely capacitive with increased power; and the phase angle moving from -90° to -180°; these changes may impact stability results. Planned future work includes developing the capability to test at higher power and over a wider frequency range, to capture these effects and use them to augment stability analyses.

IX. Conclusions and Future Work

This paper contains the first-ever impedance measurements performed on loads and sources at the NASA GRC NEAT facility, including measurements on numerous electric machines, drives, DC supplies, and resistive load banks, connected over long leads. This is a companion to the paper describing impedance measurements performed in NASA's SPEED Testbed [2].

First, an overview of the NEAT facility configuration at the time of testing is presented, and specifics of the impedance measurement process, including the hardware, measurement approach, and testing limitations, are discussed. Next, detailed source and load testing configurations are discussed; measured impedance data for the loads and sources is presented; and a load impedance model of the NEAT power system is developed and compared to the measured impedance data. Finally, a stability analysis of the NEAT EPS is performed and discussed.

Limitations to the performed measurements, including restrictions to power levels and test frequencies, are also discussed. Planned future work includes development of equipment to enable wider frequency and higher power measurement capability, as discussed in [4], and repeating the measurements and analysis described in this paper.

Acknowledgments

The authors would like to acknowledge the contributions of the staff of the NEAT facility at the Glenn Research Center (GRC) Armstrong Test facility for their contributions, including modifying the faculty and assisting during the measurements; and members of GRC's Intelligent Control and Autonomy Branch (LCC) for operating the facility while the measurements were taken. Additionally, the authors would like to thank the Advanced Air Transport Technology (AATT) Project, the Electrified Powertrain Flight Demonstration (EPFD) Project, and the Revolutionary Vertical Lift Technology (RVLT) Project for supporting this work.

References

[1] J. M. Haglage and T. W. Brown, "NASA Electric Aircraft Testbed (NEAT) Reconfiguration to Enable Altitude Testing of Megawatt-Scale Electric Machines," in AIAA Propulsion and Energy Forum, New Orleans, LA, 2020.

[2] Dever, Timothy P, Sadey, David J., Hunker, Keith R., Xavier Collazo, Patrick Hanlon, Casey Theman, Brian P. Malone, "Impedance Measurements of Motor Drive and Supply in SPEED Testbed", 2023 AIAA/IEEE Electric Aircraft Technologies Symposium (EATS).

[3] Sachs-Wetstone, Jonah J. et al., "Hybrid-Electric Aero-Propulsion Controls Testbed Results," 2023 AIAA Aviation/EATS Conference, San Diego, CA

[4] Sadey, David J. et. al., "NASA Advanced Reconfigurable Electrified Aircraft Laboratory (AREAL)", 2023 AIAA/IEEE Electric Aircraft Technologies Symposium (EATS).

[5] Kascak, Peter, Timothy Dever, and Ralph H. Jansen. "Electric Aircraft Propulsion Power System Impedance Modelling Methodology." 2021 AIAA/IEEE Electric Aircraft Technologies Symposium (EATS). IEEE, 2021.

[6] Dever, Timothy P., Peter E. Kascak, and Ralph H. Jansen. "Megawatt Electric Aircraft Propulsion Power System Impedance Modelling." 2022 IEEE Transportation Electrification Conference & Expo (ITEC). IEEE, 2022.